# Active Brownian Particle Dynamics at High Densities

A. Liluashvili, T. Voigtmann

published in

**NIC Symposium 2018**
K. Binder, M. Müller, A. Trautmann (Editors)

Forschungszentrum Jülich GmbH,
John von Neumann Institute for Computing (NIC),
Schriften des Forschungszentrums Jülich, NIC Series, Vol. 49,
ISBN 978-3-95806-285-6, pp. 313.
http://hdl.handle.net/2128/17544

# Active Brownian Particle Dynamics at High Densities

**Alexander Liluashvili**[1] **and Thomas Voigtmann**[1,2]

[1] Institut für Materialphysik im Weltraum,
Deutsches Zentrum für Luft- und Raumfahrt (DLR) e.V., 51170 Köln, Germany
*E-mail:* {*alexander.liluashvili,thomas.voigtmann*}*@dlr.de*

[2] Physik-Department, Heinrich-Heine Universität Düsseldorf,
Universitätsstraße 1, 40225 Düsseldorf, Germany

Active Brownian particles are a model system that allows physicists to understand the principles of self-propelled motion of swimming microorganisms, and also to study generic principles of motion far from thermal equilibrium. Sufficiently dense systems can kinetically arrest into a disordered state where long-range motion of individual particles is suppressed. This state is called the active glassy state. We have developed a theoretical approach to study the interplay of steric hindrance and active motion close to kinetic arrest, based on the mode-coupling theory of the glass transition. Due to the coupling between increasingly slowly relaxing collective density fluctuations and the individual swimming directions of the particles, the numerical solution of evolution equations derived within the theory becomes a formidable numerical task. We report on results obtained with the help of JURECA's computing facilities.

## 1 Introduction

Active processes play a central role in the physics of living matter. The term refers to processes that convert energy from a reservoir into useful work and hence allow biological systems to perform their tasks instead of slowly degrading into a well-mixed equilibrium of its ingredients[1]. A specific example are microswimmers, i.e., micrometer-sized entities that move by some internal self-propulsion mechanism, be they bacteria or cells or models thereof. One of the central aims of biophysics research that has emerged in the past years, is to understand generic physical principles of active motion[2,3]. Since active motion is, by its very definition, a process far from thermal equilibrium, this poses a challenge to extend the concepts of equilibrium statistical physics to strongly driven non-equilibrium systems.

Active Brownian particles (ABP) comprise a versatile model system that allows to address generic aspects of driven matter[4]. In the ABP model, suspended colloidal particles undergo Brownian motion due to equilibrium thermal fluctuations in the solvent, as well as driven motion due to some propulsion process that does not need to be specified in its details. The model can be realised in well-controlled experiments using so-called colloidal "Janus particles". ABP systems show many intriguing properties already at low and intermediate densities[5–7], for example active stresses and pressure and motility-induced phase separation (a genuine non-equilibrium phase transition induced by active motion).

At high densities, simulations have shown ABP to arrest into glassy states, i.e., disordered states that appear structurally fluid, but dynamically solid-like[8,9]. It is believed that the collective arrest (sometimes also referred to as "jamming" in this context) is important for certain patho-physiological signals or for wound healing[10–12]. Studying the influence of active motion on kinetic arrest also offers the perspective to further understand non-equilibrium driven many-body systems in general[13–15]. This prompts the development of theoretical approaches for high-density active-particle systems.

## 2 Theory

### 2.1 Mode-Coupling Theory

The simplest theoretical description of the ABP system is to consider, in two spatial dimensions, $N$ spherical particles (labelled $i = 1, \dots N$) in a volume $V$, whose positions $\vec{r}_i$ are subject to random Brownian motion, interaction forces $\vec{F}_i$ due to the other particles, and a drift velocity $v_0\vec{o}(\theta_i)$ along the intrinsic orientation of the particle, $\vec{o}(\theta) = (\cos\theta, \sin\theta)^T$. The orientations are subject to independent random thermal fluctuations, thus

$$\dot{\vec{r}}_i(t) = \vec{f}_i^r(t) + \vec{F}_i(t)/\zeta + v_0\vec{o}(\theta_i(t))\,, \qquad \dot{\theta}_i(t) = \Omega_i^r(t)\,, \tag{1}$$

where $\zeta$ is a friction coefficient characterising the solvent. $\vec{f}_i^r$ and $\Omega_i^r$ are white-noise random velocities and angular velocities whose strength is governed by the equilibrium fluctuation-dissipation theorem, $\langle \vec{f}_i^r(t)\vec{f}_j^r(t')\rangle = 4D_t\delta(t-t')\delta_{ij}$ and $\langle \Omega_i^r(t)\Omega_j^r(t')\rangle = 2D_r\delta(t-t')\delta_{ij}$ where $D_t = k_BT/\zeta$. We consider ABP with hard-disk-like direct interactions. The particle diameter $\sigma$ and $D_t$ serve to set the units of length and time. The model then has three relevant parameters: the density expressed as a dimensionless packing fraction $\phi = (\pi/4)(N/V)\sigma^2$, the orientational diffusion coefficient $D_r$, and the self-propulsion velocity $v_0$ (where $v_0 = 0$ is the "passive" case). The parameter $D_r$ controls the persistence of the motion, since orientations will randomise over a time scale $1/D_r$.

The statistical information on the dynamics of the system is encoded in the dynamical density correlation functions, $S_{ll'}(\vec{q},t) = \langle \delta\varrho_l^*(\vec{q},0)\delta\varrho_{l'}(\vec{q},-t)\rangle$, formed with the Fourier-transformed fluctuating densities $\delta\rho_l(\vec{q}) = \sum_{k=1}^N \exp[i\vec{q}\cdot\vec{r}_k]\exp[il\theta_k]/\sqrt{N}$. By a projection-operator formalism, one can derive evolution equations for the transient density correlation functions (where the angular brackets are an average over the equilibrium Boltzmann ensemble). One gets, in obvious matrix notation[16]

$$\boldsymbol{\omega}_{T,\vec{q}}^{-1}\cdot\dot{\boldsymbol{S}}(\vec{q},t) + \boldsymbol{W}_{\vec{q}}\cdot\boldsymbol{S}(\vec{q},t) + \int_0^t dt'\,\boldsymbol{m}(\vec{q},t-t')\cdot\Big(\dot{\boldsymbol{S}}(\vec{q},t') + \boldsymbol{\omega}_R\cdot\boldsymbol{S}(\vec{q},t)\Big) = \boldsymbol{0}\,, \tag{2}$$

where $\boldsymbol{\omega}_{T,R}$ and $\boldsymbol{W}$ are known prefactors. Eq. 2 is a relaxation equation where the memory kernel $\boldsymbol{m}(\vec{q},t)$ that describes delayed friction is a correlation function of reduced fluctuating forces. In the approximation of mode-coupling theory,

$$m_{ll'}(\vec{q},t) \approx \frac{N}{2V}\int\frac{d^2k}{(2\pi)^2}\sum_{l_1l_2l_1'l_2'}\mathcal{V}^\dagger_{ll_1l_2}(\vec{q},\vec{k},\vec{p})S_{l_1l_1'}(\vec{k},t)S_{l_2l_2'}(\vec{p},t)\mathcal{V}_{l'l_1'l_2'}(\vec{q},\vec{k},\vec{p})\,, \tag{3}$$

where $\vec{q} = \vec{k} + \vec{p}$. The coupling coefficients $\mathcal{V}$ and $\mathcal{V}^\dagger$ can be calculated in terms of the equilibrium static structure factors of the system. Activity enters $\mathcal{V}^\dagger$ through an additive term proportional to $v_0\sigma/D_t$; for the explicit formulas, we refer to Ref. 16. Of interest in the following is the positional density correlation function $S_{00}(q,t)$; it depends on the wave vector only through the magnitude $q = |\vec{q}|$ as long as the system is statistically homogeneous and isotropic.

The density correlation functions allow to distinguish fluid-like from glassy arrested states: in the fluid, density fluctuations all eventually decay, $\lim_{t\to\infty}\boldsymbol{S}(\vec{q},t) = \boldsymbol{0}$. At high densities, the equations admit a solution where $\lim_{t\to\infty}\boldsymbol{S}(\vec{q},t) = \boldsymbol{F}(\vec{q}) \neq \boldsymbol{0}$. This defines the idealised glass: a solid state, where a finite memory remains of an initial density fluctuation for arbitrarily long times. The points in parameter space where the long-time limit

of the solution jumps, are the glass transition points identified by the theory. Approaching the glass transition from the liquid-state side, the decay of the correlation function $\boldsymbol{S}(\vec{q},t)$ is characterised by a structural relaxation time $\tau$ that diverges at the transition.

### 2.2 Numerics

Solving Eqs. 2 and 3 numerically presents a challenge: close to the glass transition, the decay of both $\boldsymbol{S}(\vec{q},t)$ and $\boldsymbol{m}(\vec{q},t)$ covers many orders of magnitude in time, so that the integro-differential equation Eq. 2 needs to be solved over a very large time interval. This requires specially adapted integration schemes that perform successive coarsening of the time-domain discretisation. Since $\boldsymbol{m}(\vec{q},t)$ is a nonlinear functional of $\boldsymbol{S}(\vec{q},t)$, solving the discretised time evolution requires, at each integration step, the solution of an implicit equation to determine the value of the correlation function. For the evaluation of the memory kernel, the integrals in wave-vector space are discretised on a regular grid of $M = 128$ (occasionally $M = 256$) wave-vector magnitudes up to a cutoff, $q\sigma \leq 50$, leading to a set of $M$ coupled nonlinear equations. Details of the algorithm can be found in Ref. 16.

For the calculation, we introduce a cutoff in angular indices, $|l| \leq L$. The simple dipolar coupling of orientations and positions in Eq. 1 suggests $L = 1$ to be reasonable. Selected runs with $L = 2$ show cutoff effects on $S_{00}(q,t)$ to be weak. With the typical choices of numerical parameters, calculation of a single set of correlation functions $S_{ll'}(\vec{q},t)$ for a given set of physical parameters $(\phi, v_0, D_r)$ close to the glass transition requires about 16 GiB RAM with $M = 256$ and takes up to 16 h using 24 cores of a single JURECA node (64 GiB RAM and up to 72 h for $L = 2$). To construct the fluid–glass state diagram, more than 15000 independent runs were needed.

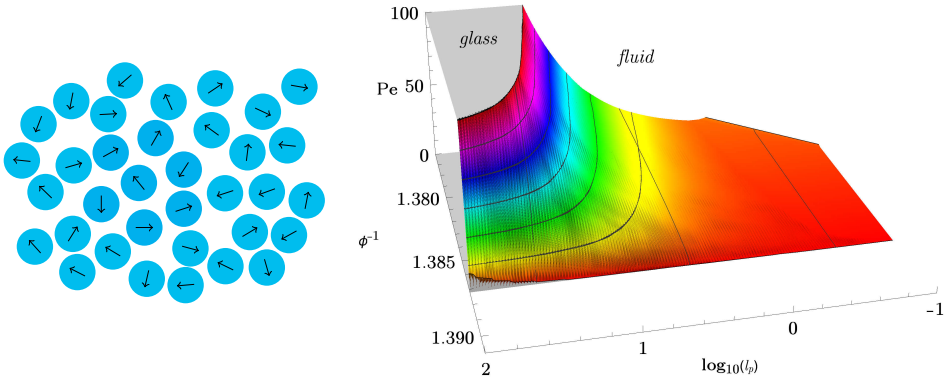


Figure 1. Left: Sketch of the active Brownian hard-disk system. Particles undergo Brownian motion (diffusion coefficient $D_t$) and swim along their internal directions with velocity $v_0$; the direction reorients randomly on a time scale $1/D_r$. Right: Glass-transition diagram. For high density (low free volume $\phi^{-1}$), low activity strength (Péclet number $Pe = v_0^2/D_r D_t$), and large persistence of swimming ($\ell_p = v_0/D_r$), the system is kinetically arrested. The surface separates these glassy disordered-solid states (below) from fluid ones (above).

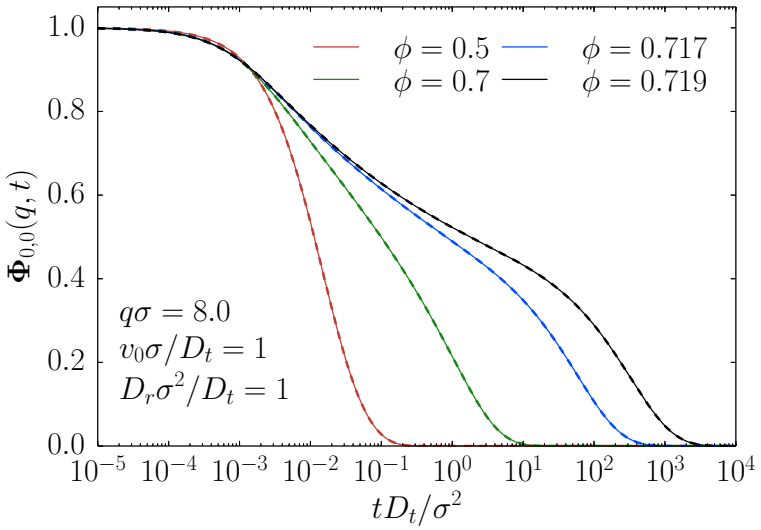


Figure 2. Normalised density correlation functions $\Phi_{00}(q,t) = S_{00}(q,t)/S_{00}(q,0)$ of an active hard-disk system with self-propulsion velocity $v_0 = 1$, at various packing fractions $\phi$ as labelled. As $\phi$ increases, collective relaxation of the ABP system becomes increasingly slow. Solid lines are results obtained from angular-index cutoff $L = 1$, dashed lines are results for $L = 2$ for comparison.

## 3 Results

### 3.1 Collective Dynamics

A common representation of the surface of glass-transition points in the three-dimensional parameter space of the spherical ABP system, is in form of a "jamming phase diagram"[12] (although kinetic arrest is not, strictly speaking, a "phase"), cf. Fig. 1. At low densities, the activity-induced changes to the dynamics of the ABP system are quantified by a single dimensionless Péclet number expressing the strength of active over passive motion, $Pe = v_0^2/D_r D_t$. But the glass-transition surface depends on both the strength of swimming, $Pe$, as well as the persistence of swimming, quantified by the persistence length $\ell_p = v_0/D_r$. This reveals an interplay of swimming with caging of particles by their neighbours.

On approaching the glass transition, the relaxation of density fluctuations in the fluid becomes increasingly sluggish. Structural relaxation proceeds in two steps: after a first short-time decay, particles are transiently caged in the environment provided by their neighbours, and this leads to an intermediate-time plateau in $S_{00}(q,t)$ that becomes increasingly pronounced the closer the system is to glassy arrest. In the liquid, a second decay of the correlations to zero on the structural-relaxation time scale $\tau$ sets in, and $\tau$ becomes increasingly large upon approaching the transition (where it diverges). This scenario is well established for the passive system upon increasing the density. In the active system, qualitatively the same scenario applies when decreasing the self-propulsion velocity at fixed packing fraction, see Fig. 2.

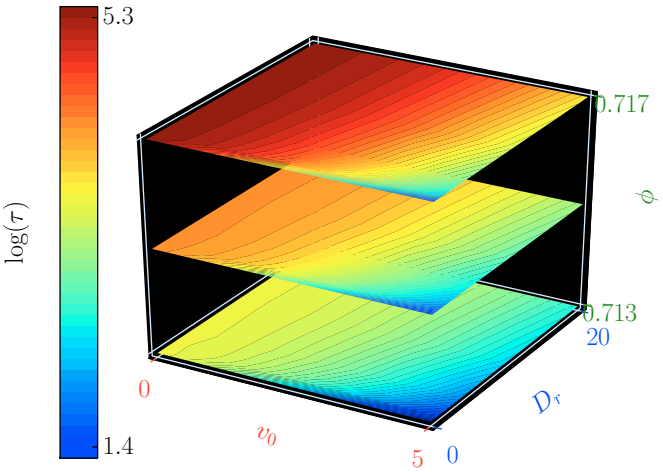


Figure 3. Structural relaxation times $\tau$ of active Brownian hard-disk systems as functions of packing fraction $\phi$, self-propulsion velocity $v_0$, and inverse persistence time $D_r$.

The structural relaxation times depend on the two parameters that enter through active driving, viz. $v_0$ and $D_r$, as is shown in Fig. 3. The overall increase of $\tau$ with increasing density reflects the universal aspects of kinetic arrest (both in passive and active systems). But no simple scaling form in terms of the Péclet number and the persistence length, as many simplified theoretical approaches to ABP would suggest, can be found in our data.

The glass transition is driven by the cage effect, and hence by density fluctuations on the length scale of interparticle distances, $q \approx 2\pi/\sigma$. In the active system, a variation of $q$ reveals further information, because the persistence length $\ell_p$ provides a second length scale[7]: at low densities, fluctuations on short length scales, $q\ell_p \gg 1$, decay due to the intrinsic Brownian motion of the particles, while long-wavelength fluctuations, $q\ell_p \ll 1$, decay due to activity-enhanced diffusion. The intermediate case $q\ell_p \approx 1$ reveals an oscillatory decay pattern: persistent motion can temporarily re-instantiate density correlations. At high densities, even in the presence of active motion, the slow dynamics is governed by the diffusive relaxation of the cages, and density correlations decay monotonically for each $q$ (left panel of Fig. 4), while oscillations in $q$ reflect the positional correlations in a dense packing. Sufficiently persistent driving, on the other hand, can dominate cage relaxation and cause an oscillatory decay of correlations to reappear (right panel). These decay patterns are ruled out for density fluctuations in an equilibrium system, and hence they highlight the non-equilibrium nature of active dynamics.

### 3.2 Tagged-Particle Dynamics

The collective density correlation functions of microswimmer systems can be difficult to measure. An experimentally easier to access quantity is the mean-squared displacement (MSD) of a single tracer particle, $\delta r^2(t) = \langle|\vec{r}_s(t) - \vec{r}_s(0)|^2\rangle$. Using colloidal particles that can be imaged by microscopy, the MSD are readily obtained and serve as dynamical

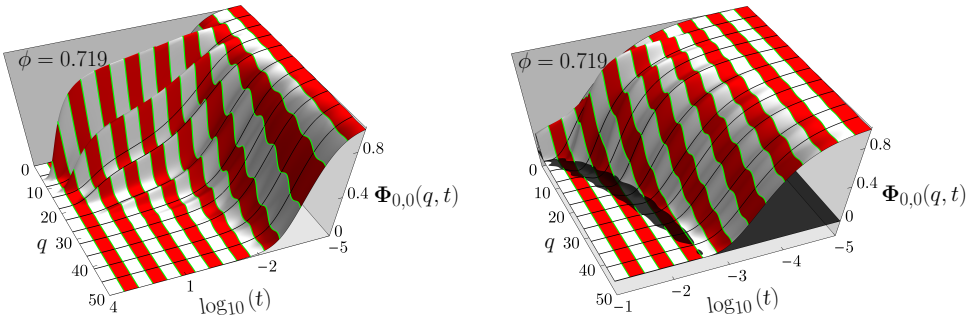


Figure 4. Normalised density correlation functions $\Phi_{00}(q,t)$ as a function of time and wave number $q$, for fixed self-propulsion velocity and fixed packing fraction. Left: Low activity case, $v_0 = 1$ with $D_r = 1$, showing pure relaxation of density fluctuations at all wave lengths. Right: High activity case, $v_0 = 48$ and $D_r = 72$, where density fluctuations on intermediate wave lengths decay non-monotonically (negative values of $S_{00}(q,t)$ indicated by a grey area) and signal a contribution from persistent swimming competing with diffusive relaxation.

probes of the suspension. The MSD can be calculated from the low-$q$ limit of the tagged-particle density correlation function $S^s_{00}(q,t) = \langle \exp[i\vec{q}\cdot(\vec{r}_s(t) - \vec{r}_s(0)]\rangle$, via the relation $\delta r^2(t) = \lim_{q\to 0}(S^s_{00}(q,t) - 1)/(q^2/4)$. Within mode-coupling theory, one writes down equations for $\boldsymbol{S}^s(\vec{q},t)$ that are similar in structure to Eqs. 2 and 3. There again appears a memory kernel to describe slow structural relaxation, and this memory kernel is a functional of $\boldsymbol{S}^s(\vec{q},t)$ and also slaved to the collective dynamics $\boldsymbol{S}(\vec{q},t)$.

Some cases of interest for experimental setups are the motion of a passive tracer in a host suspension of active particles, i.e., $v_0 \neq 0$ and $v_0^s = 0$. As expected, the long-time diffusion of the passive tracer is enhanced by the activity of the host suspension (left panel of Fig. 5). In this sense, a passive tracer can be used to quantify the active motion of, say, a bacterial suspension. The reversed case, an active tracer in a passive dense suspension, $v_0 = 0$ and $v_0^s \neq 0$, models the case of bacteria swimming in viscoelastic fluids. Again, increasing the activity enhances the long-time diffusion (right panel of Fig. 5). But compared to the speed-up experienced by a passive tracer in an active suspension, the increased activity of a single particle swimming in a dense passive suspension is rather weak.

## 4 Concluding Remarks

We have solved numerically the equations of motion for dense suspensions of active Brownian particles in two dimensions that were recently derived in the framework of mode-coupling theory[16]. The solution of these equations is numerically highly demanding, because active motion couples orientational and translational modes of motion in the dense system, introduces a further length scale through the persistence length, and because structural relaxation is nontrivial over many orders of magnitude in time.

The dynamics of dense active Brownian particle systems is an interplay between caging and swimming, i.e., between the steric hindrance between particles that governs the passive system, and the active-motion induced weakening of the cages of neighbouring particles. At sufficiently high density, an "active glass" region appears in the state diagram, where cage relaxation becomes ineffective even in the presence of swimming.

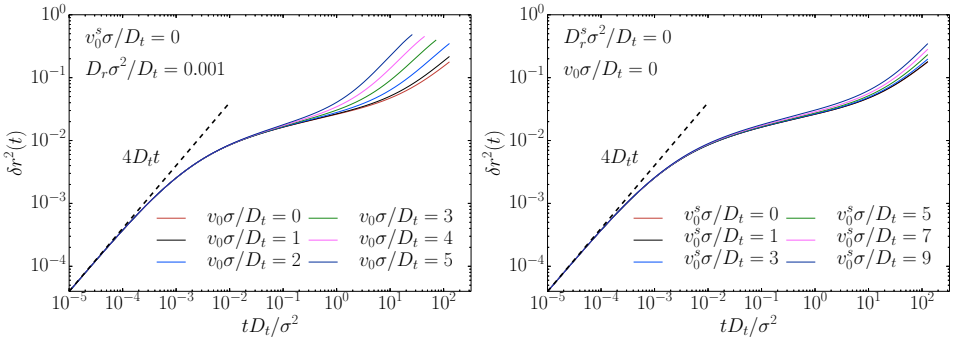


Figure 5. Mean-squared displacements (MSD) in dense suspensions with activity: the left panel shows the MSD for a passive tracer particle in a dense suspension of active particles, for increasing activity of the host suspension (curves right to left). The right panel shows the MSD of an active particle swimming in a dense passive suspension close to the glass transition (increasing single-particle activity for curves from right to left).

While the low-density dynamics of ABP is governed by a single activity strength (a single Péclet number), the high-density dynamics displays a separate dependence on both the strength and the persistence of swimming. Although all density-fluctuations modes to all length scales arrest simultaneously, the persistence length for large swimming velocities also separates a regime of short-wavelength passive Brownian-diffusive relaxation from one of large-wavelength active-diffusive relaxation. There appears an intermediate regime where the persistent motion leads to genuine non-equilibrium relaxation patterns that are not captured in quasi-equilibrium approaches to ABP.

The transient density correlation functions that we have calculated form the basis for calculations of non-equilibrium transport coefficients. Within an integration-through transients (ITT) formalism, generalisations of Green-Kubo integrals can be derived that are valid for arbitrarily strong perturbations from equilibrium. If one considers active motion as such a strong perturbation, it becomes possible by the combination of ITT and MCT to calculate, for example, coarse-grained self-propulsion velocities of active systems. Such transport coefficients are the basis for coarse-grained theories that describe, for example, motility-induced phase separation of active-particle systems. ITT-MCT thus provides a possible route to arrive at coarse-grained descriptions of active systems systematically by starting from the microscopic equations of motion.

We have also presented first results based on MCT for the dynamics of active swimmers in passive suspensions and, vice versa, the dynamics of passive tracers in an active fluid. The theory thus allows to discuss how the enhancement of structural relaxation by activity can conveniently be measured by observation of passive tracers in the active system, or how swimmers behave in non-trivial solvents where they face molecular crowding.

## Acknowledgements

We thank J. Ónody for help in developing the theory, and J. Ónody and J. Reichert for a critical reading of the manuscript. We gratefully acknowledge funding from Deutsche Forschungsgemeinschaft (DFG SPP 1726 “Microswimmers”, Vo 1270/7) and the comput-

ing time granted by the John von Neumann Institute for Computing (NIC) and provided on the supercomputer JURECA[17] at Jülich Supercomputing Centre (JSC), project HKU26.

## References

1. P. Nelson and M. Radosavljevic, *Biological Physics*, Freeman, New York, USA, 2000.
2. M. E. Cates, *Diffusive transport without detailed balance in motile bacteria: does microbiology need statistical physics?*, Rep. Prog. Phys., **75**, 042601, 2012.
3. S. Ramaswamy, *Active matter*, J. Stat. Mech., **17**, 054002, 2017.
4. P. Romanczuk, M. Bär, W. Ebeling, B. Lindner, and L. Schimansky-Geier, *Active Brownian particles*, Eur. Phys. J.: Special Topics, **202**, 1–162, 2012.
5. J. Elgeti, R. G. Winkler, and G. Gompper, *Physics of microswimmers–single particle motion and collective behavior: a review*, Rep. Prog. Phys., **78**, 056601, 2015.
6. A. Zöttl and H. Stark, *Emergent behavior in active colloids*, J. Phys.: Condens. Matter, **28**, 253001, 2016.
7. C. Kurzthaler, S. Leitmann, and T. Franosch, *Intermediate scattering function of an anisotropic active Brownian particle*, Sci. Rep., **6**, 36702, 2016.
8. R. Ni, M. A. Cohen Stuart, and M. Dijkstra, *Pushing the glass transition towards random close packing using self-propelled hard spheres*, Nature Commun., **4**, 2704, 2013.
9. Y. Fily, S. Henkes, and M. C. Marchetti, *Freezing and phase separation of self-propelled disks*, Soft Matter, **10**, 2132–2140, 2013.
10. K. D. Nnetu, M. Knorr, J. Käs, and M. Zink, *The impact of jamming on boundaries of collectively moving weak-interacting cells*, New J. Phys., **14**, 115012, 2012.
11. M. Sadati, N. T. Qazvini, R. Krishnan, C. Y. Park, and J. J. Fredberg, *Collective migration and cell jamming*, Differentiation, **86**, 121–125, 2013.
12. D. Bi, X. Yang, M. C. Marchetti, and M. L. Manning, *Motility-Driven Glass and Jamming Transitions in Biological Tissues*, Phys. Rev. X, **6**, 021011, 2016.
13. L. Berthier and J. Kurchan, *Non-equilibrium glass transitions in driven and active matter*, Nature Phys., **9**, 310–314, 2013.
14. L. Berthier, *Nonequilibrium Glassy Dynamics of Self-Propelled Hard Disks*, Phys. Rev. Lett., **112**, 220602, 2014.
15. G. Szamel, *Theory for the dynamics of dense systems of athermal self-propelled particles*, Phys. Rev. E, **93**, 012603, 2015.
16. A. Liluashvili, J. Ónody, and Th. Voigtmann, *Mode-coupling theory for active brownian particles*, Phys. Rev. E, **96**, 062608, 2017.
17. Jülich Supercomputing Centre, *JURECA: General-purpose supercomputer at Jülich Supercomputing Centre*, Journal of large-scale research facilities, **2**, no. A62, 2016.